

## ASSESSMENT OF FATIGUE CRACK GROWTH DATA AVAILABLE FOR THE AA6061-T651 USING A LOCAL STRAIN-BASED APPROACH

Alfredo S. Ribeiro, [aribeiro@utad.pt](mailto:aribeiro@utad.pt)

José A.F.O. Correia, [jcorreia@utad.pt](mailto:jcorreia@utad.pt)

Abílio M.P. de Jesus, [ajesus@utad.pt](mailto:ajesus@utad.pt)

Engineering Department, School of Sciences and Technology, University of Trás-os-Montes and Alto Douro, Vila Real, Portugal  
LAETA/UCVE, IDMEC-P6lo FEUP, Porto, Portugal

**Abstract.** *Fatigue crack growth models based on elastic-plastic stress-strain histories, at the crack tip vicinity, and strain-life damage models have been proposed. The UniGrow model fits this particular class of fatigue crack propagation models. The residual stresses developed at the crack tip play a central role in these models, since they are used to assess the actual crack driving force, taking into account mean stress and loading sequential effects. The performance of the UniGrow model is assessed based on available experimental constant amplitude crack propagation data, derived for the 6061-T651 aluminum alloy. Key issues in fatigue crack growth prediction, using the UniGrow model, are discussed, in particular the residual stresses evolution. Using available strain-life data, it was possible to model the crack propagation behavior for the AA6061-T651, taking into account the stress R-Ratio effects. A satisfactory agreement between the predictions and the experimental crack propagation data was found.*

**Keywords:** AA6061-T651, Local Strain approach, Crack propagation, UniGrow model.

### 1. INTRODUCTION

The research on fatigue of materials and structures has deserved great interest both by academia and industry. Fatigue has been investigated for more than 150 years and still is a hot topic in research (Schütz, W., 1996). In particular, the investigation on fatigue crack propagation is not fully accomplished, despite the great developments achieved in the last decades. Paris (Paris *et al.*, 1961) is considered the first one to establish a direct correlation between the fatigue crack propagation and a Fracture Mechanics parameter – the stress intensity factor, leading to the so-called Paris's law. Since then, the Paris' law has been used extensively to model fatigue crack growth under constant amplitude loading. However, the Paris's law shows several limitations, namely it only models the stable crack propagation, excluding near threshold and near unstable crack propagation regimes. Also, the stress ratio effects are not accounted in the Paris's law. Many other fatigue crack propagation laws have been proposed to overcome the limitations of the Paris's law and also to deal with variable amplitude loading (Beden *et al.*, 2009). The proposed fatigue models differ on the number of variables involved and the number of parameters required to be identified by curve fitting.

Local strain-based approaches to fatigue (Coffin, 1954, Manson, 1954, Morrow, 1965, Smith *et al.*, 1970) have been assumed as an alternative to Fracture Mechanics based fatigue crack propagation models. Local strain-based approaches to fatigue are often applied to model the crack initiation on notched components (Shang *et al.*, 2001). Some authors (Glinka, 1985, Peeker and Niemi, 1999, Noroozi *et al.*, 2005, 2007, 2008, Hurley and Evans, 2007) have proposed a relation between the local strain-based approaches to fatigue and the Fracture Mechanics based fatigue crack propagation models. They assume crack propagation as a process of continuous re-initializations (failure of consecutive representative materials elements). The resulting crack propagation model has been demonstrated to be able of correlation of crack propagation data from several sources, including the stress ratio effects. The crack tip stress-strain fields are computed using elastoplastic analysis and fracture mechanics concepts which are used together a fatigue damage law to predict the failure of representative material elements. The simplified methods of Neuber (1961) and Glinka (Moslski and Glinka, 1981) are used to compute the elastoplastic stress field at the crack tip vicinity using the elastic stress distribution given by the Fracture Mechanics concepts (Noroozi *et al.*, 2005) (Moftakhar *et al.*, 1995) (Reinhard *et al.* 1997).

The application of local strain approaches on modeling fatigue crack propagation has the important advantage of requiring a smaller amount of experimental data than usually demanded Fracture Mechanics approaches. Also, experimental fatigue crack propagation data is more expensive to obtain, since the crack propagation tests are more time consuming and usually several stress ratios are expected to be tested. The interrelation between the local strain approaches and Fracture Mechanics also opens the possibility for a unify approach for modeling crack initiation and propagation.

This paper proposes the assessment of the model proposed recently by Noroozi *et al.* (2005, 2007) to model fatigue crack propagation, based on the local strain approach to fatigue. This model has been denoted as UniGrow model and it has been classified as a residual stress based crack propagation model (Mikheevskiy and Glinka, 2009). The model is applied to derive the fatigue crack propagation data for the 6061-T651 aluminum alloy, for distinct stress R-ratios.

Results are compared with the available experimental data. The required strain-life data was obtained by the authors and was already published in the literature (Ribeiro *et al.* 2005, 2007, 2009). The representative material element size is assessed. Also, the residual stress field is analyzed for distinct crack sizes and stress R-Ratios. The elastoplastic stresses at the vicinity of the crack tip, computed using simplified formulae, are compared with the stresses computed using an elastoplastic finite element analysis of the specimen used in the experimental program to derive the crack propagation data. The analytical models proposed by Noroozi *et al.* (2005, 2007) to compute the elastoplastic stress/strain distribution ahead of the crack tip may lead to inconsistent residual stress distribution since the proposed analytical approaches do not account for stress redistribution due to yielding. The present paper proposes, alternatively, the use of elastoplastic finite element in order to obtain a more accurate prediction of the residual stress distribution. The accurate prediction of the residual stress distribution is of primordial importance for the application of the UniGrow model, since the model is a residual stress-based propagation model. The stress ratio effects, on crack propagation rates, are partially modeled by the level and extension of the compressive residual stresses.

## 2. OVERVIEW OF THE UNIGROW MODEL

The UniGrow model was proposed by Noroozi *et al.* (2005) based on the following assumptions:

- The material is composed of elementary particles of a finite dimension  $\rho^*$ . It represents an elementary material block size, below which material cannot be regarded as a continuum, Fig. 1a.
- The fatigue crack tip is considered equivalent to a notch with radius  $\rho^*$ , Fig. 1b.
- The fatigue crack growth process is considered as successive crack increments due to crack re-initiations over the distance  $\rho^*$ .
- The fatigue crack growth rate can be determined as:

$$\frac{da}{dN} = \frac{\rho^*}{N_f} \quad (1)$$

where  $N_f$  is the number of cycles required to fail the material over the distance  $\rho^*$ , which can be determined using the Smith–Watson–Topper (Smith *et al.*, 1970) fatigue damage parameter:

$$\sigma_{max} \frac{\Delta\varepsilon}{2} = \frac{(\sigma'_f)^2}{E} (2N_f)^{2b} + \sigma'_f \varepsilon'_f (2N_f)^{b+c} \quad (2)$$

The maximum stress  $\sigma_{max}$  and the strain range  $\Delta\varepsilon$  have to be evaluated as the average values at the elementary material block size,  $\rho^*$ , taking into account an elastoplastic analysis.

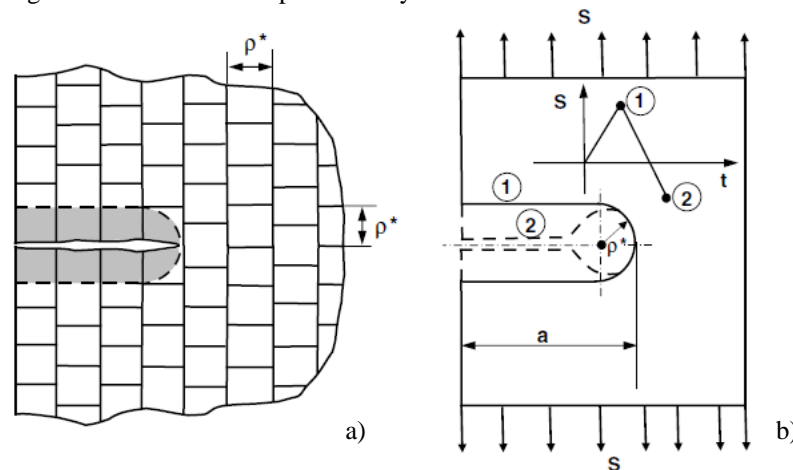


Figure 1. Crack configuration according to the UniGrow model: a) crack and the discrete elementary material blocks; b) crack shape at the tensile maximum and compressive minimum loads (Noroozi *et al.* 2005).

To compute the elastoplastic stresses and strains at the elementary material blocks ahead of the crack tip, the numerical procedure proposed by Noroozi *et al.* (2005, 2007) was followed in this paper:

- The elastic stresses are computed ahead of the crack tip using the Creager-Paris (Creager and Paris, 1967) solution for a crack with a tip radius  $\rho^*$ , using the applied stress intensity factors.
- The actual elastoplastic stresses and strains, ahead of the crack tip, are computed using the Neuber or Glinka's approaches (Neuber, 1961) (Mosliski and Glinka, 1981). Multiaxial approaches were adopted in this paper using the procedures presented by Moftakhar *et al.* (1995) and Reinhard *et al.* (1997).
- The residual stress distribution ahead of the crack tip is computed using the actual elastoplastic stresses computed at the end of the first load reversal and subsequent cyclic elastoplastic stress range,  $\sigma_r = \sigma_{max} - \Delta\sigma$ .
- The residual stress distribution computed ahead of the crack tip is assumed to be applied on crack faces, behind the crack tip, in a symmetric way. The residual stress intensity factor,  $K_r$ , is computed using the weight function method (Glinka, 1996).
- The applied stress intensity factor (maximum and range values) is corrected using the residual stress intensity value, resulting the total values,  $K_{max,tot}$  and  $\Delta K_{tot}$ .
- Using the total values of the stress intensity factors, the first and second steps before are repeated to determine the corrected values for the maximum actual stress and actual strain range at the material representative elements. Then, equations (2) and (1) are applied to compute the crack growth rate.

The described methodology does not allow close-form solutions for the crack propagation rates. However, introducing some simplifications about the elastoplastic conditions (e.g. predominantly elastic behavior) it is possible to derive close-form solutions for the crack propagation rates based on a two-parameters crack driving force (Noroozi *et al.* 2005, 2007):

$$\frac{da}{dN} = C \left[ (K_{max,tot})^p (\Delta K_{tot})^q \right]^\gamma \quad (3)$$

where  $C$ ,  $p$  and  $\gamma$  are constants to be correlated with the cyclic constants of the material in a form depending on the elastoplastic conditions at the crack tip. In this paper, the full solution of the methodology proposed by Noroozi *et al.* (2005) is followed.

Besides the elastoplastic cyclic and fatigue properties of the material, the UniGrow model requires the definition of the elementary material block size,  $\rho^*$ . This parameter can be estimated using the fatigue endurance limit  $\Delta\sigma_f$  and the fatigue crack propagation threshold,  $\Delta K_{th}$  (Noroozi *et al.*, 2005). However, and since these values are not available for the material under investigation, an iterative process is used to compute  $\rho^*$ . This parameter is computed using a try and error procedure in order a good correlation of the experimental crack growth data is obtained.

### 3. FATIGUE DATA OF THE 6061-T651 ALUMINIUM ALLOY

The 6061-T651 aluminum alloy has been investigated by the authors (Ribeiro *et al.*, 2005, 2007, 2009), regarding the fatigue behavior characterization. This section presents the main results which are required for the application of the UniGrow model. The cyclic elastoplastic behavior was characterized as well as the strain-life fatigue data using smooth and polished cylindrical specimens. The fatigue crack propagation rates are also characterized using cracked specimens, in particular the Compact Tension (CT) specimens.

#### 3.1. Strain-life fatigue data

Smooth and polished cylindrical specimens ( $\phi 8$  mm) were tested under strain control conditions (strain ratio equal to -1) according to the ASTM E606 standard (ASTM, 1998). Using the stabilized cyclic behavior, the cyclic curve of the material was represented in Fig. 2. This curve represents the relation between the stabilized stress amplitude and the plastic strain amplitude. The Morrow's relation (Morrow, 1965) is also included in Fig. 2, resulting the strain hardening

coefficient  $K' = 393.4 \text{ MPa}$  and the strain hardening exponent  $n' = 0.0567$ . Figure 3 represents the strain-life data, which includes the Coffin-Manson (Coffin, 1954) (Manson, 1954) and Basquin (1910) relations. The fatigue strength coefficient  $\sigma'_f$  results equal to 394 MPa and the fatigue strength exponent  $b$  results equal to  $-0.0453$ . The fatigue ductility coefficient  $\epsilon'_f$  is equal to  $0.8680$  and the fatigue ductility exponent  $c$  is equal to  $-0.7745$ . The fatigue strength coefficient was computed using the Young's modulus equal to 68 GPa.

### 3.2. Fatigue crack propagation data

In order to determine the fatigue crack propagation curves ( $da/dN$  versus  $\Delta K$  curves) for the 6061-T651 aluminum alloy, CT specimens were used. Specimens with a thickness  $B=10$  mm and nominal width  $W=50$  mm were cut from a base plate with a thickness of 24 mm. These dimensions are according to the recommendations of the ASTM E647 standard (ASTM, 2000). Figure 4 illustrates the crack growth data derived for the 6061-T651 aluminum alloy, for two stress ratios, namely  $R=0.1$  and  $R=0.5$ . The crack growth rates can be satisfactorily correlated by a power law, as proposed by Paris (Paris *et al.*, 1961), individually for each stress ratio. The crack propagation is clearly influenced by the stress ratio. Higher the stress ratios results in higher crack growth ratios.

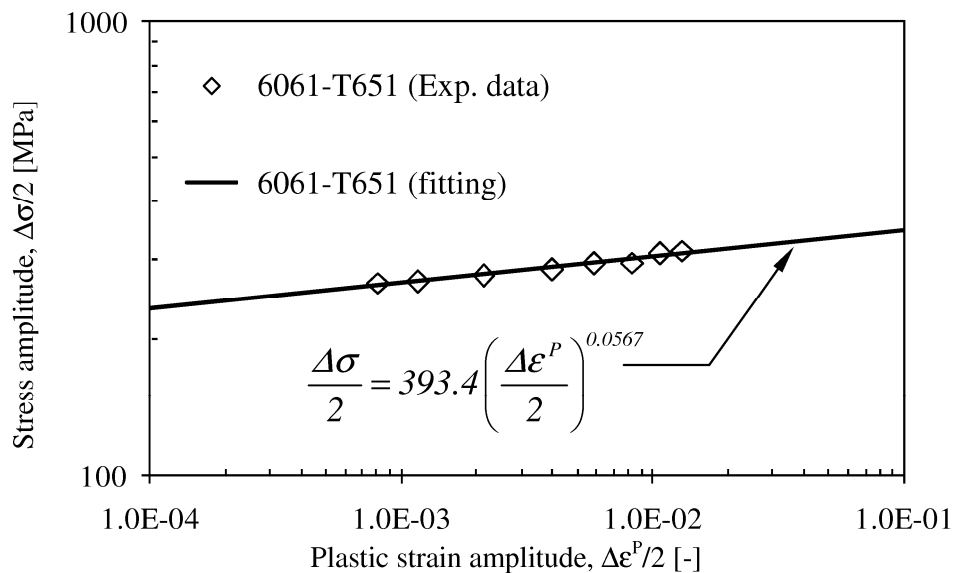


Figure 2. Cyclic curve of the 6061-T651 aluminum alloy.

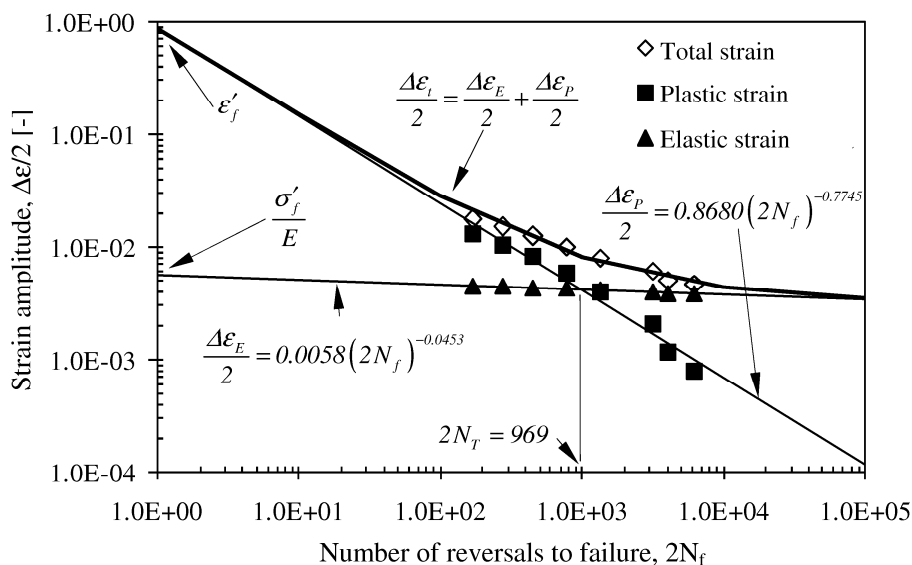


Figure 3. Strain-life fatigue data of the 6061-T651 aluminum alloy.

#### 4. RESULTS AND DISCUSSION

The UniGrow model was implemented in the Microsoft Excel<sup>®</sup> supported on VBA programming, taking into account the CT geometry. The input data are the material properties, loads, dimensions of the CT specimen, including the initial and final crack size to be simulated. Additionally, the elementary material block size,  $\rho^*$ , is required. This parameter was evaluated by a try and error procedure, in order the numerical results agree satisfactorily with the experimental data. Two possibilities for the elastoplastic analysis at the crack vicinity are allowed, namely using the Neuber and Glinka's approaches. A multiaxial approach was used as referred in section 2. In order to compute the residual stress distribution ahead the crack front, stresses were computed at points equally spaced according distances smaller than  $\rho^*$ . This concern was taken into account in order to prevent the influence of the discretization on the residual stress distribution and particularly on computed residual stress intensity factor, given by weight function method. A discretization of  $\rho^*/10$  was found suitable.

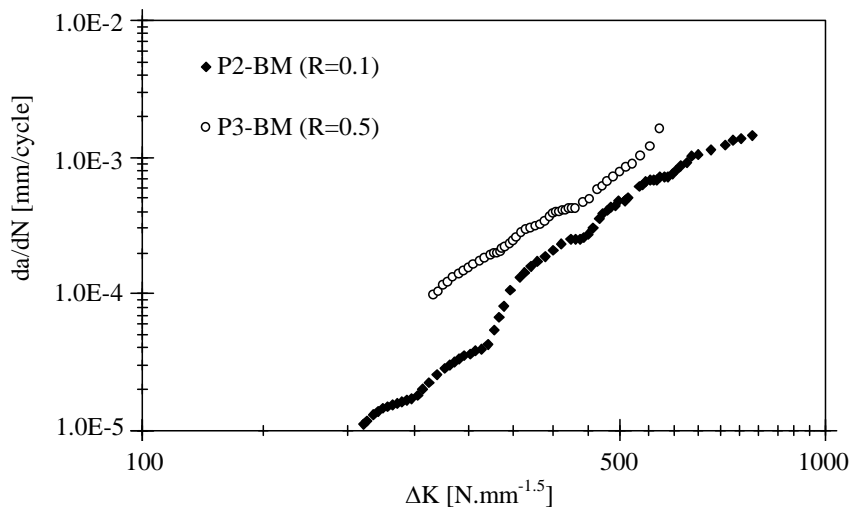


Figure 4. Crack propagation data of the 6061-T651 aluminum alloy.

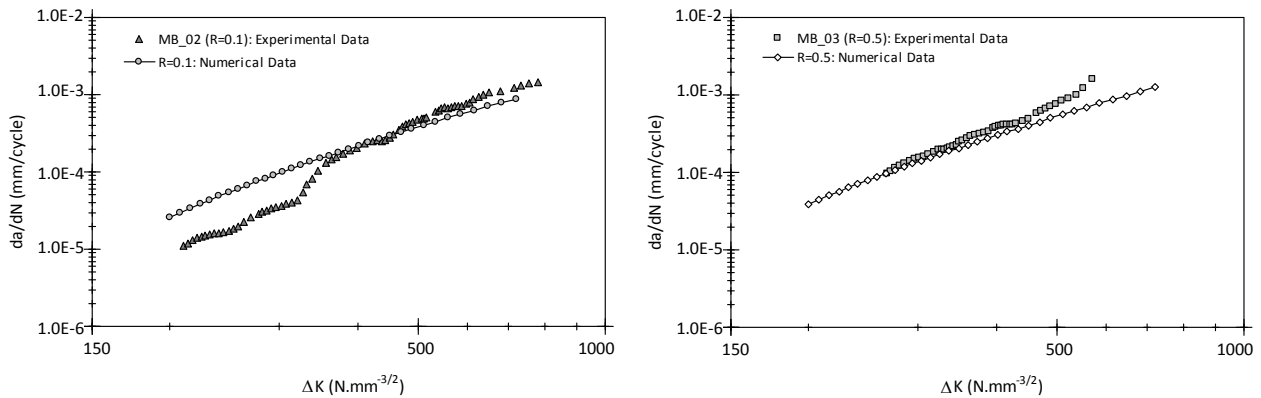


Figure 5. Experimental crack growth data and UniGrow predictions for the AA 6061-T651.

Figure 5 presents the predictions of the fatigue crack growth rates for each stress ratio, using the multiaxial Neuber's approach for the elastoplastic analysis. Satisfactory predictions were obtained for  $\rho^* = 2E-5$  m. Noroozi *et al.* (2007) proposed a value for  $\rho^*$  equal to  $8E-6$  m, for the 2024-T351 aluminum alloy, which is about the same order of magnitude. The experimental results show, for  $R=0.0$ , a sudden increase ("jump") in the crack growth rate for  $\Delta K$  within the range  $300-400$   $N.mm^{-1.5}$ . The slope of the crack growth data before and after the jump is approximately the same, which strengthens the idea of an abnormal behavior. Therefore, the  $\rho^*$  was identified taking into account the crack propagation data, for  $R=0.1$ , after the jump. In order to illustrate the effect of the stress ratio on fatigue crack growth rates, Fig. 6 plots the fatigue crack growth rates for several stress ratios. The predicted fatigue crack propagation curves are essentially parallel to each other and the increase in the crack propagation rates is more significant for higher stress ratios. The model takes into account the stress ratio effects in two ways, namely using the SWT parameter and also

through the compressive residual stresses, which are subtracted from the stress range to derive the total stress intensity factor range, lower than the applied one. The compressive residual stresses tend to vanish for high stress ratios, which make the crack growth rates to increase, as illustrated by Fig. 6.

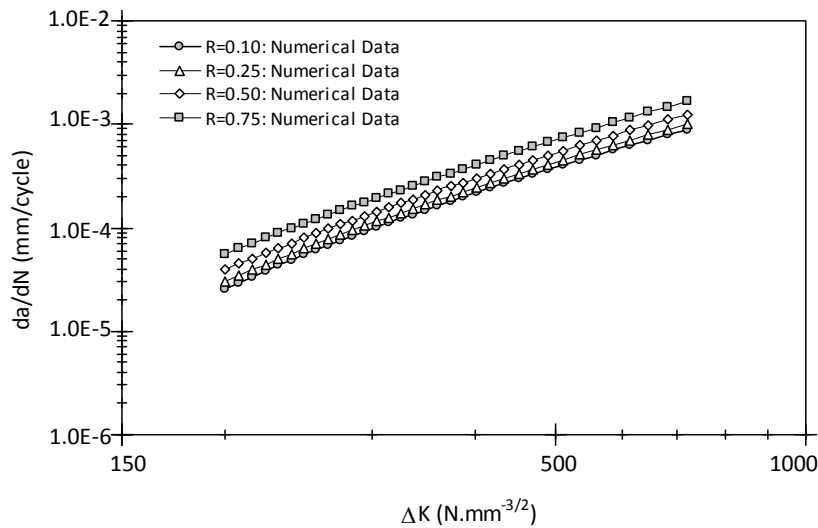


Figure 6. Fatigue crack growth predictions for the AA6061-T651 for distinct stress R-Ratios.

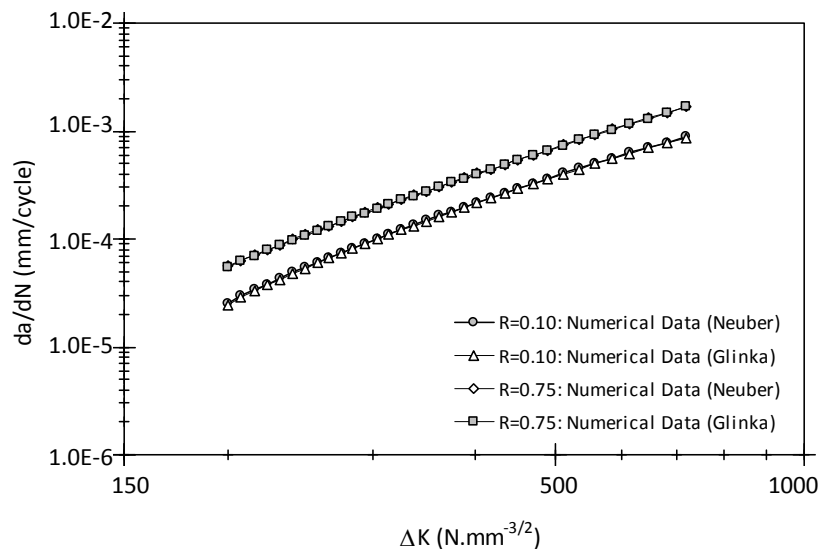


Figure 7. Fatigue crack growth predictions for the AA6061-T651 for distinct stress R-ratios, supported on Neuber and Glinka's approaches.

Figure 7 shows the crack growth predictions which resulted from the application of the elastoplastic analyses according the Neuber and Glinka's approaches. Despite the Neuber's approach being usually considered to give an upper bound for the elastoplastic stresses and the Glinka's approach a lower bound (Reinhard *et al.*, 1997), the final results for the crack growth rates are essentially the same for both analyses.

The elastoplastic analysis at the crack front is a key step of the UniGrow model. The accuracy of the elastoplastic analysis is crucial in a correct crack propagation modeling. In this paper, the application of the UniGrow model is based on a simplified elastoplastic analysis based on the multiaxial Neuber or Glinka's approach. In order to assess the accuracy of the simplified elastoplastic analysis, a bi-dimensional finite element model of the CT specimen is built and used in the elastoplastic analysis. A very refined mesh at the crack tip region is required, in order to model the crack tip notch radius,  $\rho^*$ . Figure 8 illustrates the finite element mesh of the CT geometry with the respective boundary conditions. Only  $\frac{1}{2}$  of the geometry is modeled, taking into account the existing symmetry plane. Plane stress conditions were assumed. The load was applied at a node located in the geometrical center of the pin. A Von Mises yield theory with multilinear kinematic hardening model was used to model the plastic behavior. The model was fitted to the cyclic

curve of the material. The simulations were carried out using the ANSYS® 12.0 code. The two stress ratios that were considered in the experimental program ( $R=0.1$  and  $R=0.5$ ) were simulated. A sequence of two load steps was simulated, namely the maximum load of 3309.2 N was firstly applied and then removed in a second load step. The resulted elastoplastic stress distributions are compared with the solutions from the analytical simplified analyses. In particular, the maximum stresses ( $\sigma_{xx}$ ,  $\sigma_{yy}$ ), at the end of the first load step, and the residual stresses, at the end of the second load step, are compared with the analytical solutions, along the distance from the crack tip and for the symmetry plane ( $y=0$  in Fig. 8).

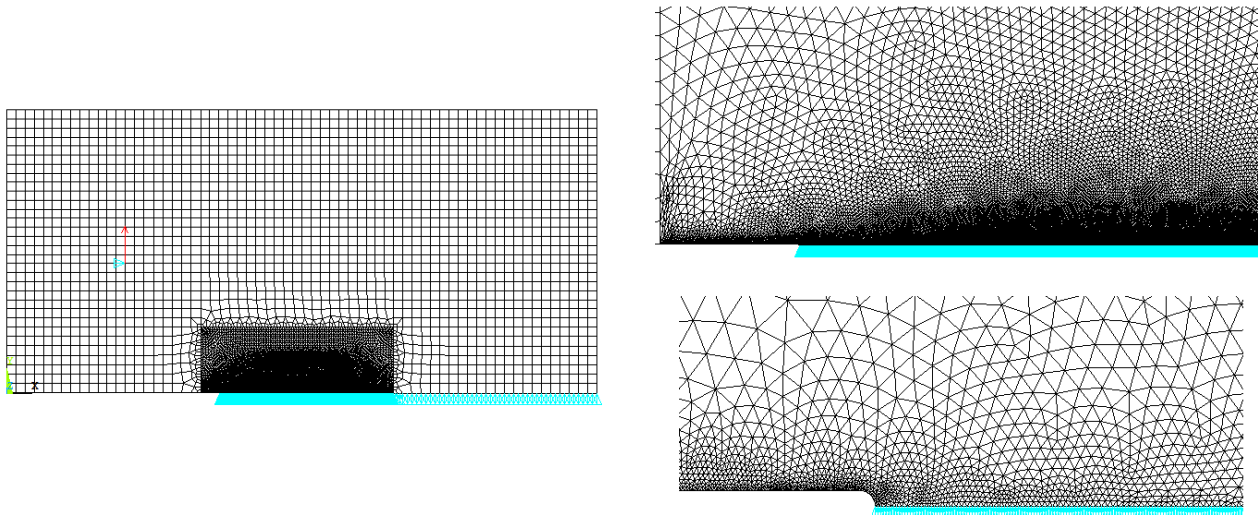


Figure 8. Finite element mesh of the CT specimen: global mesh and boundary conditions (left) and zoom of the mesh around the crack tip (right).

Figure 9 compares the analytical and numerical distributions of the maximum elastoplastic stresses obtained for the CT specimen, for  $a=10$  mm. The analytical solutions used were based on Neuber and Glinka's approaches. These two solutions yields very similar results for both  $\sigma_{xx}$  and  $\sigma_{yy}$  stresses. The numerical results agree satisfactorily with the analytical results, this agreement being better for  $\sigma_{xx}$ . Figure 10 shows the residual stress distributions, for the  $y$  direction (load direction). Again, the two analytical models give approximately the same results. They predict compressive stress distributions which are only slightly affected by the stress  $R$ -ratio. The numerical model foresees a narrower compressive stress distribution. Furthermore, the compressive stress distribution is more sensitive to the stress  $R$ -ratio and become more localized as the stress ratio increases, which means that the compressive residual stress intensity factor tends to zero, as the stress ratio increases above 0.5. This condition is consistent with the conclusions proposed by Noroozi *et al.* (2005, 2007).

## 5. CONCLUSIONS

The UniGrow model, which uses the local strain-life approach to model the crack propagation, was applied to predict the fatigue crack propagation of the 6061-T651 aluminum alloy. Experimental strain-life and fatigue crack propagation data was derived for the aluminum alloy, by authors, and used in the analysis. The UniGrow model produced satisfactory predictions of the crack propagation data, predicting the stress ratio effects, with a representative material element of  $2 \times 10^{-5}$  m. This representative material element shows approximately the same order of magnitude of the values proposed in literature for other aluminum alloys. Therefore, the results of the present paper further validate the UniGrow model, which was proposed recently Glinka and his co-workers.

A simplified analytical procedure for elastoplastic analysis at the crack tip region was adopted, namely based on multiaxial Neuber and Glinka's rules. Despite the well known upper bound stress values given by the Neuber's approach, both approaches gave very similar stress distributions and crack propagation rates. A finite element model of the CT specimen was built for elastoplastic analysis in order to verify the elastoplastic stresses from the analytical solutions. In general, a good agreement was observed for the maximum elastoplastic stresses. However, for the residual compressive stress distribution deviations are observed, which increases for higher stress ratios. It seems that the analytical models overestimate the residual stresses for high stress ratios. This is an important conclusion of this work, since the UniGrow model is a residual stress -based propagation model, which means that the stress ratio effects are modeled, in part, by the level of compressive residual stresses. The proposed analytical models are not able to simulate the stress redistribution due to yielding. Therefore, they are recommended for computation of the elastoplastic

stress/strains at the notch root only. The residual stress distribution should be computed by elastoplastic finite element analysis as proposed in this paper.

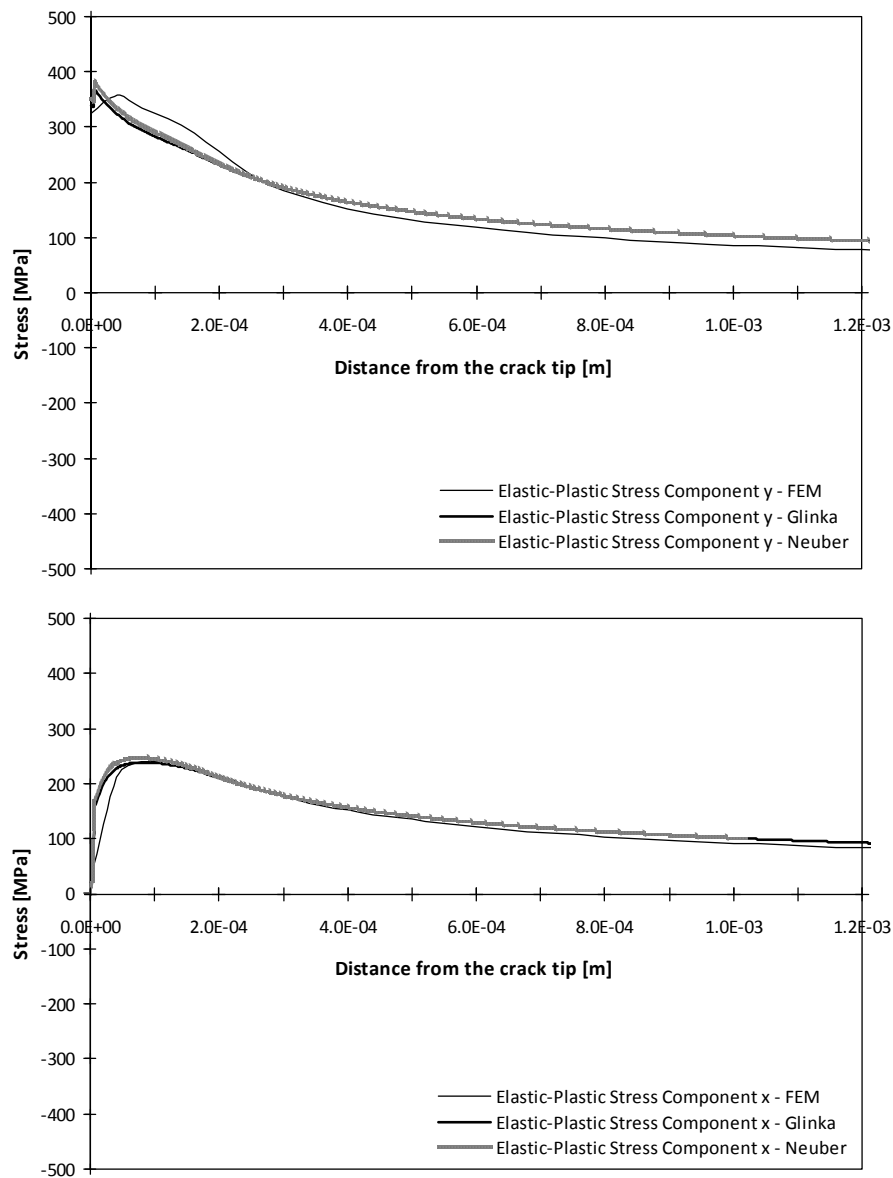


Figure 9. Comparison of numerical and analytical stress distributions for the CT geometry with  $a=10$  mm and  $F_{max}=3309.2$  N.



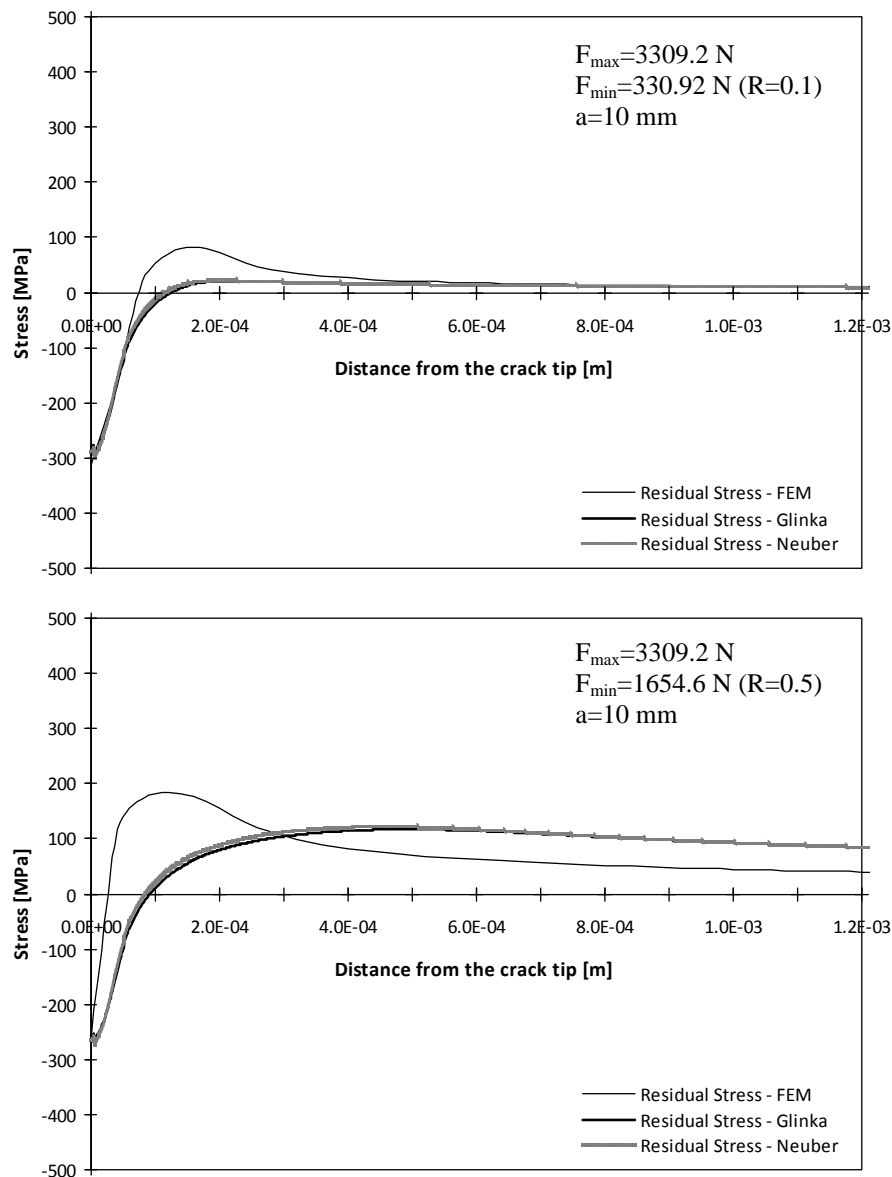


Figure 10. Comparison of numerical and analytical residual stress distributions for the CT geometry under two distinct stress ratios.

## 6. REFERENCES

- ASTM, 1998, "ASTM E606: Standard Practice for Strain-Controlled Fatigue Testing", Annual Book of ASTM Standards, Vol. 03.01, ASTM, West Conshohocken, PA, USA.
- ASTM, 2000, "ASTM E647: Standard Test Method for Measurement of Fatigue Crack Growth Rates", Annual Book of ASTM Standards, Vol. 03.01, ASTM, West Conshohocken, PA, USA.
- Basquin, O. H., 1910, "The Exponential Law of Endurance Tests", Proceedings of ASTM, 10 (II), pp. 625-630.
- Beden, S.M., Abdullah, S., Ariffin, A.K., 2009, "Review of Fatigue Crack Propagation Models for Metallic Components", European Journal of Scientific Research, Vol.28, pp.364-397
- Coffin, L.F., 1954, "A study of the effects of the cyclic thermal stresses on a ductile metal", Translations of the ASME, Vol. 76, pp. 931-950.
- Creager, M., Paris, P.C., 1967, "Elastic field equations for blunt cracks with reference to stress corrosion cracking", International Journal of Fracture Mechanics, Vol.3, pp.247-52.
- Glinka, G., 1985, "A notch stress-strain analysis approach to fatigue crack growth", Engineering Fracture Mechanics, Vol. 21, pp.245-261.

- Glinka, G. 1996, "Development of weight functions and computer integration procedures for calculating stress intensity factors around cracks subjected to complex stress fields", Progress Report No.1, Stress and Fatigue-Fracture Design, Petersburg Ontario, Canada.
- Hurley, P.J., Evans, W.J., 2007, "A methodology for predicting fatigue crack propagation rates in titanium based on damage accumulation, Scripta Materialia, Vol. 56, pp.681-684.
- Manson, S.S., 1954, "Behaviour of materials under conditions of thermal stress", NACA TN-2933, National Advisory Committee for Aeronautics.
- Mikheevskiy, S., Glinka, G., 2009, "Elastic-plastic fatigue crack growth analysis under variable amplitude loading spectra", International Journal of Fatigue, Vol. 31, pp. 1828-1836.
- Moftakhar, A., Buczynski, A., Glinka, G., 1995, "Calculation of elasto-plastic strains and stresses in notches under multiaxial loading", International Journal of Fracture, Vol. 70, pp. 357-373.
- Molski, K., Glinka, G., 1981, "A method of elastic-plastic stress and strain calculation at a notch root", Materials Science and Engineering, Vol. 50, pp. 93-100.
- Morrow, J. D., 1965, "Cyclic plastic strain energy and fatigue of metals", Int. Friction, Damping and Cyclic Plasticity, ASTM, STP 378, pp. 45-87.
- Neuber, H., 1961, "Theory of stress concentration for shear-strained prismatic bodies with arbitrary nonlinear stress-strain law". Trans ASME Journal of Applied Mechanics, Vol. 28, pp. 544-551.
- Noroozi, A.H., G. Glinka, and S. Lambert, 2005, "A two parameter driving force for fatigue crack growth analysis", International Journal of Fatigue, Vol. 27, pp. 1277-1296.
- Noroozi, A.H., G. Glinka, and S. Lambert, 2007, "A study of the stress ratio effects on fatigue crack growth using the unified two-parameter fatigue crack growth driving force", International Journal of Fatigue, Vol. 29, pp. 1616-1633.
- Noroozi, A.H., G. Glinka, and S. Lambert, 2008, "Prediction of fatigue crack growth under constant amplitude loading and a single overload based on elasto-plastic crack tip stresses and strains", Engineering Fracture Mechanics, Vol. 75, pp. 188-206.
- Paris, P.C., Gomez, M., Anderson, W.E., 1961, "A rational analytic theory of fatigue", Trend Engineering, Vol.13, pp.9-14.
- Pecker, E., Niemi, E., 1999, "Fatigue crack propagation model based on a local strain approach", Journal of Constructional Steel Research, Vol. 49, pp. 139-155.
- Reinhard, W., Moftakhar, A., Glinka, G., 1997, "An Efficient Method for Calculating Multiaxial Elasto-Plastic Notch Tip Strains and Stresses under Proportional Loading" Fatigue and Fracture Mechanics: 27<sup>th</sup> Volume, ASTM STP 1296, R.S. Piascik, J.C. Newman, N.E. Dowling, Eds., American Society for Testing and Materials, pp. 613-629.
- Ribeiro, A.S., Borrego, L.P., Jesus, A.M.P., Costa, J.D.M., 2009, "Comparison of the low-cycle fatigue properties between the 6082-T6 and 6061-T651 aluminium alloys", In: Proceedings of 20th International Congress of Mechanical Engineering (COBEM 2010), Gramado, RS, Brazil, 15-20 November, 2009.
- Ribeiro, A.S., Jesus, A.M.P., Fernandes, A.A., 2005, "Fatigue crack propagation rates of the aluminium alloy 6061-T651", In: Proceedings of 18th International Congress of Mechanical Engineering, Ouro Preto, MG, Brasil, 6-11 November, 2005.
- Ribeiro, A.S., Jesus, A.M.P., Fernandes, A.A., 2007, "comportamento elastoplástico cíclico e à fadiga da liga de alumínio 6061 - T651, Revista Iberoamericana de Ingeniería Mecánica, Vol. 11, pp. 53-65.
- Schütz, W., 1996. "A History of Fatigue", Engineering Fracture Mechanics, Vol. 54, pp. 263-300.
- Shang, D.-G., Wang, D.-K., Li, M., Yao, W.-X., 2001, "Local stress-strain field intensity approach to fatigue life prediction under random cyclic loading", International Journal of Fatigue, Vol. 23, pp. 903-910.
- Smith, K. N., Watson, P., Topper, T. H., 1970, "A Stress-Strain Function for the Fatigue of Metals", Journal of Materials, Vol. 5, No. 4, pp. 767-778.

## 7. RESPONSIBILITY NOTICE

The authors are the only responsible for the printed material included in this paper.